Structural Accommodation of Osmium Tetroxide in Tertiary Butanol Solution

S. Díaz Moreno[†] and D. T. Bowron*[,‡]

European Synchrotron Radiation Facility, B.P. 220, 6 rue Jules Horowitz, 38043 Grenoble Cedex 9, France, and ISIS Facility, CLRC Rutherford Appleton Laboratory, Chilton, Didcot OX11 0QX, U.K.

Received: March 19, 2002; In Final Form: June 20, 2002

The structure of a 0.053 mol fraction solution of osmium tetroxide (OsO_4) in tertiary butanol ($(CH_3)_3COH$) has been investigated by H/D isotope substitution neutron scattering methods. The three intermolecular correlations of interest, solute−solute, solvent−solvent, and solute−solvent, have been investigated by means of an empirical potential structure refinement of the experimental data. The picture of the system to emerge from the analysis is one in which the OsO_4 molecules are generally seen to be well dispersed throughout the liquid as individual, i.e., nonaggregated, solutes. The solute favors a local environment where it is surrounded by the polar hydroxyl groups of the alcohol molecules but manages to accommodate itself without destroying the quantitative extent of the interalcohol hydrogen bonding that takes place, when compared with the pure solvent. Qualitatively, however, some modification of the hydrogen bond network between the alcohol molecules is seen to occur, largely through a small increase in the length of the inter-alcohol hydrogen bond and also through an increase in the breadth of the distribution.

Introduction

Osmium tetroxide, OsO_4, is an important chemical compound that has a wide range of uses, i.e., as a staining and fixation agent in the examination of biological tissue components by electron microscopy[1] or as the most reliable reagent available for the cis hydroxylation of alkenes to give the corresponding cis-diols.[2] Commercially, when not supplied as a pure compound, it is most commonly available in aqueous or alcoholic (tertiary butanol) solution because much of the compound's subsequent chemistry is often performed in such solvents.[3] In this study, we present an investigation of the structure of a dilute solution, 0.053 mol fraction, of osmium tetroxide in tertiary butanol, with the aim of providing a baseline study of a liquid-state chemical environment in which this compound is active.

Tertiary butanol is an ideal solvent for this study because a detailed understanding of its liquid state structure has recently been achieved.[4−6] The findings of these baseline studies showed that the structure of this liquid alcohol is determined through a fine balance between the degree of nonpolar to nonpolar contacts mediated by the three alcohol methyl groups and the interalcohol molecule hydrogen bonding interactions mediated by the single alcohol hydroxyl group. In particular, the recent experimental studies showed that the latter polar group interaction is considerably less dominant than previous computer simulation based investigations had suggested.[7,8]

Of interest in this particular study is the identification of the local environment that is favored by the OsO_4 molecules as this is likely to play an important role in the reaction mechanisms that can be supported in the solvent medium. A particular question that this study attempts to address is whether the OsO_4 molecule favors the nonpolar environment offered by the methyl group mediated alcohol−alcohol interactions or whether better in-solution accommodation can be found in the vicinity of the polar hydroxyl groups in the liquid. Also, it is interesting to determine how the inclusion of this compound into the liquid alcohol modifies the solvent molecule interactions with themselves.

Here, we utilize the technique of second-order difference neutron scattering to probe the structure of this solution.[9−12] This technique takes advantage of the different scattering properties for neutrons of hydrogen and deuterium to allow us to vary the scattering contrast of the alcohol molecules in the system and then, through scattering difference methods, determine in great detail the nature of the intermolecular interactions. To maximize the information extracted from the experimental data, the technique of empirical potential structure refinement[13] has been applied which effectively allows us to produce an ensemble of model structures that reproduce the salient features of the experimental scattering data. These models are then interrogated to extract information on all of the atomic site−site partial pair distribution functions, the spatial distribution of the molecules, and their relative orientations.

Experiment

To extract the structural correlation functions from the alcohol solution, the technique of neutron diffraction with H/D isotope substitution was used. Three measurements on isotopically different, but chemically identical, mixtures were made. These mixtures were (1) 0.053 mol fraction OsO_4 in $(CH_3)_3COD$, (2) 0.053 mol fraction OsO_4 in a 1:1 mixture of $(CH_3)_3COD$ and $(CD_3)_3COD$, and (3) 0.053 mol fraction OsO_4 in $(CD_3)_3COD$. The isotopic substitution has thus effectively been performed on the methyl hydrogen sites of the alcohol molecule.

Following standard methods,[4,9,10] these three solutions provide us with access to detailed information weighted toward the intermolecular correlations between the alcohol methyl hydrogen sites. The set of measurements allows us to extract three partial structure factors for analysis $S_{HH}(Q)$, $S_{XH}(Q)$, and $S_{XX}(Q)$, where Q is defined as the magnitude of the momentum transfer vector of the scattered neutrons. These three partial structure factors

* To whom correspondence should be addressed. E-mail: D. T.Bowron@rl.ac.uk.

[†] European Synchrotron Radiation Facility.

[‡] CLRC Rutherford Appleton Laboratory.

10.1021/jp025789+ CCC: $22.00
Published on Web 10/23/2002

TABLE 1: Relative Intermolecular Scattering Weights for a 0.053 mol Fraction Solution of Osmium Tetroxide in Tertiary Butanol[a]

	$S_{HH}(Q)$ Intermolecular Weights					
	M			M 1.0000		
	$S_{XH}(Q)$ Intermolecular Weights					
	CC	C	O	D	OS	OO
M	0.1624	0.4871	0.1417	0.1629	0.0145	0.0315
	$S_{XX}(Q)$ Intermolecular Weights					
	CC	C	O	D	OS	OO
CC	0.0264					
C	0.1582	0.2373				
O	0.0460	0.1380	0.0201			
D	0.0529	0.1587	0.0461	0.0265		
OS	0.0047	0.0141	0.0041	0.0047	0.0002	
OO	0.0102	0.0307	0.0089	0.0103	0.0009	0.0010

[a] Hydrogen/deuterium substitution has been performed on the alcohol methyl hydrogen sites; that is, experiments were performed on (i) $(CH_3)_3COD$ with 0.053 mol fraction OsO_4, (ii) 1:1 mixture of $(CH_3)_3COD$ and $(CD_3)_3COD$ with 0.053 mol fraction OsO_4, and (iii) $(CD_3)_3COD$ with 0.053 mol fraction OsO_4. For the alcohol molecule, CC refers to the central carbon atom, C refers to each of the methyl group carbon atoms, M refers to a methyl group hydrogen, O refers to the alcohol hydroxyl group oxygen, and D refers to the alcohol hydroxyl group hydrogen. For the osmium tetroxide, OS refers to the osmium atom sites in OsO_4 and OO to the oxygen atom sites on that molecule.

respectively relate to (i) the correlations between the isotopically labeled atomic sites alone, (ii) the correlations between the isotopically labeled sites and the nonlabeled atomic sites in the mixture, and (iii) the correlations between the atomic sites that have not been labeled. The weightings relating to the three experiments giving the three sets of partial structure factors are given in Table 1. By maintaining the isotopic composition of the hydroxyl group hydrogen site as deuterium, a choice made to optimize the composition for neutron scattering experiments, no corrections for in-solution isotopic exchange needed to be made for the mixture sample. The methyl group hydrogen sites do not undergo in-solution atomic exchange with the hydroxyl site deuterium atoms or with themselves, and in consequence, Table 1 shows that the function $S_{HH}(Q)$ only contains correlations involving the methyl group hydrogen atoms.

In all subsequent discussion, the following labels have been assigned to the distinguishable atomic sites on the tertiary butanol molecules and osmium tetroxide molecules. On the alcohol molecules, CC refers to the central carbon atom, C refers to each of the methyl group carbon atoms, M refers to a methyl group hydrogen, O refers to the hydroxyl group oxygen, and D refers to the hydroxyl group hydrogen site, which as mentioned above was always deuterated. On the OsO_4 molecule, OS refers to the osmium atoms and OO refers to each of the four oxygen atoms in the molecule.

Because of the toxicity of OsO_4, handling of the compound was kept to a minimum, and the samples were prepared by adding the contents of as-supplied preweighed ampules containing 500 mg of OsO_4 (Sigma-Aldrich), to appropriate quantities of the isotopically labeled alcohol. The solutions were then transferred to a titanium−zirconium alloy cell for the neutron scattering measurement. The composition of this cell corresponds to a zero coherent scattering neutron cross section ($Ti_{0.68}Zr_{0.32}$), and thus, the cell does not contribute to the structural signal measured from the sample. The cell dimensions were 1 mm × 35 mm × 35 mm. Diffraction data were collected on the SANDALS instrument at the ISIS pulsed neutron facility of the Rutherford Appleton Laboratory, U.K. All measurements were made at room temperature ~25 °C. SANDALS was selected for these measurements as it is specifically optimized for the measurement of samples containing significant quantities of light elements such as hydrogen. The combination of data collection at small scattering angles <40° and the use of high-energy neutrons minimizes the effects of inelastic scattering processes which can be difficult to correct. At the time of this experiment, SANDALS was operating with eighteen banks of detectors covering an angular range from 3.5° to 37°. Data analysis was performed using the ATLAS analysis suite of computer programs, and corrections were made for instrument background, cell scattering, neutron absorption, and multiple scattering, with all data normalized to the incoherent scattering level of vanadium.[11] Throughout this process, data corresponding to the scattering of neutrons with wavelengths in the range 0.12−3.0 Å were used, avoiding the need to correct for neutron absorption resonances of osmium that could otherwise have affected the data. The final corrections for inelasticity and the calculation of the isotope substitution partial structure factors was performed by the techniques outlined by Soper and Luzar.[12]

Theory

After appropriate corrections, a single neutron scattering experiment on a polyatomic liquid system measures a function called the total structure factor. This is defined as

$$F(Q) = \sum_{\alpha\beta} c_\alpha c_\beta b_\alpha b_\beta (S_{\alpha\beta}(Q) - 1) \qquad (1)$$

where the summation is over all atom pairs in the sample, and c_α and c_β are the atomic fractions of species α and β, b_α and b_β are their coherent neutron scattering lengths, and $S_{\alpha\beta}(Q)$ are the partial structure factors that result from the interatomic structural correlations between atom pairs α and β. Q as previously mentioned, is the magnitude of the momentum transfer vector of the scattered neutrons and is defined as $Q = 4\pi/\lambda$ (sin θ), where 2θ is the scattering angle and λ is the wavelength of the scattered neutrons. These partial structure factors are related to the partial pair distribution functions $g_{\alpha\beta}(r)$ and are given by the well-known Fourier transform relationship:

$$S_{\alpha\beta}(Q) - 1 = 4\pi\rho \int r^2 [g_{\alpha\beta}(r) - 1] \frac{\sin(Qr)}{Qr} \, dr \qquad (2)$$

where ρ is the average atomic number density of the sample. Naturally, if only one experiment is performed to give the total structure factor for a sample, it is only possible to extract the total pair distribution function of atoms in the system, i.e., the sum of all of the partial pair distribution functions. This can be an extremely difficult function to interpret.

As previously discussed, the essence of the H/D isotopic substitution second order difference neutron scattering technique is the experimental separation of the total structure factor into three terms of interest, $S_{HH}(Q)$, $S_{XH}(Q)$, and $S_{XX}(Q)$. These functions are determined by solving the following set of simultaneous equations, corresponding to the scattering that is measured for each of the three samples described in the Experimental Section above:

$$F_H(Q) = c_X^2 b_X^2 [S_{XX}(Q) - 1] + 2c_X c_H b_X b_H [S_{XH}(Q) - 1] + c_H^2 b_H^2 [S_{HH}(Q) - 1] \qquad (3)$$

$$F_{HD}(Q) = c_X^2 b_X^2 [S_{XX}(Q) - 1] + 2c_X c_H b_X b_{HD} [S_{XH}(Q) - 1] + c_H^2 b_{HD}^2 [S_{HH}(Q) - 1] \qquad (4)$$

$$F_D(Q) = c_X^2 b_X^2 [S_{XX}(Q) - 1] + 2c_X c_H b_X b_D [S_{XH}(Q) - 1] + c_H^2 b_D^2 [S_{HH}(Q) - 1] \quad (5)$$

where

$$c_X = \sum_{\alpha \neq H} c_\alpha \quad (6)$$

$$b_X = \sum_{\alpha \neq H} \frac{c_\alpha b_\alpha}{c_X} \quad (7)$$

$$c_H = (1 - c_X) \quad (8)$$

$$b_{HD} = x b_H + (1 - x) b_D \quad (9)$$

The subscript X collectively refers to every atom type that is not isotopically substituted in the experiments. The subscripts H, D, and HD refer to hydrogen, deuterium, and mixture of hydrogen and deuterium respectively, and x is the fraction of light hydrogen in the mixture sample. In the experiment described here, x has a value of 0.5 as the mixture sample is a 1:1 molecular ratio of protiated and deuterated tertiary butanol.

Once determined, these composite partial structure factors, $S_{HH}(Q)$, $S_{XH}(Q)$, and $S_{XX}(Q)$, are in turn related to the partial pair distribution functions $g_{HH}(r)$, $g_{XH}(r)$, and $g_{XX}(r)$, by the same Fourier transform as given in eq 2. In effect, they represent a considerable clarification of the contributions that go to make up the total atomic pair distribution functions. In a conventional analysis of diffraction data, the structural information contained in these composite partial distribution functions, would be extracted by an examination of the positions and widths of the various peaks. The distribution of these peaks relates to distribution of interatomic distances present in the system under investigation. In addition, for a given partial distribution function $g_{\alpha\beta}(r)$, the areas beneath the peaks are related to coordination numbers, i.e., the number of atoms of type β, that can be found in the distance range between r_1 and r_2 about atoms of type α. This can be evaluated by calculating

$$(N_\beta^{(\alpha)})_{r1}^{r2} = 4\pi\rho c_\beta \int_{r1}^{r2} r^2 g_{\alpha\beta}(r)\, dr \quad (10)$$

Rather than adopt a conventional analysis scheme, here we proceed by using these data as input to an advanced computer modeling process.

Data Analysis

To maximize the structural information that can be extracted from the experimental data, analysis was performed using the empirical potential structure refinement technique developed by A. K.Soper.[13,14] This method combines Monte Carlo computer modeling procedures with constrained structure refinement against the measured experimental data, to produce an ensemble of model structures that satisfy the neutron partial structure factors. This ensemble of model structures is then interrogated to extract any quantity of structural interest, i.e., the full set of interatomic partial pair distribution functions, the intermolecular orientational correlation functions,[15] and spatial density functions.[16] In effect, this procedure uses computational methods to find acceptable solutions to the atomic distribution functions that characterize the liquid, which, by default, must satisfy the fundamental constraints of atomic density, chemical composition, and basic molecular geometries.

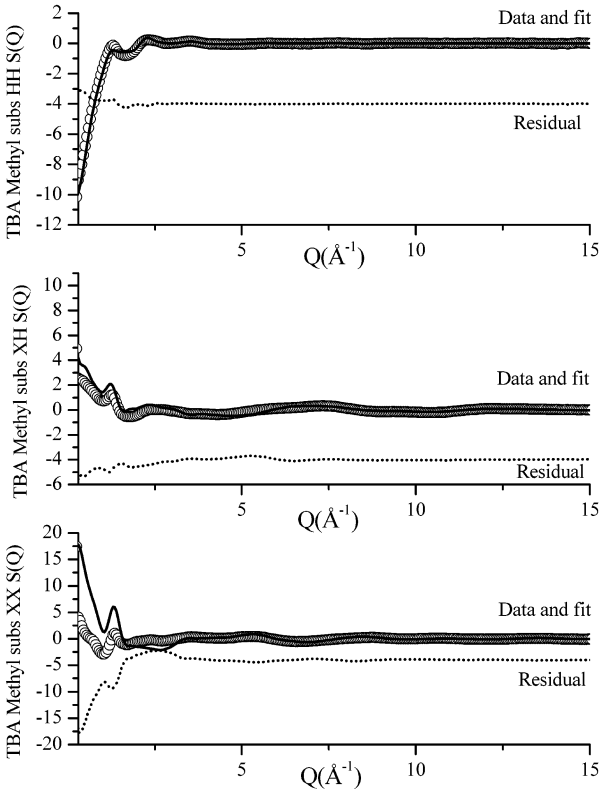

Figure 1. Experimental data (circles) and EPSR fits (solid lines) to the partial structure factors derived from H/D isotope substitution neutron scattering measurements performed on the alcohol methyl group hydrogen sites, in 0.053 mol fration solution of osmium tetroxide in tertiary butanol at room temperature. From top to bottom are shown $S_{HH}(Q) - 1$, $S_{XH}(Q) - 1$, and $S_{XX}(Q) - 1$ after correction for backgrounds, multiple scattering and absorption of neutrons, scaling to the incoherent scattering of vanadium, and removal of self-scattering and neutron inelastic scattering contributions. The fit residuals are also shown (broken lines offset by -4 units).

The EPSR procedure was initialized using a cubic box of side length 25.6 Å containing 108 tertiary butanol molecules and 6 OsO_4 molecules, corresponding to an atomic density of 0.098 atom Å^{-3}. The structures of the molecules within this box are constrained to remain consistent with the known form of the tertiary butanol and osmium tetroxide molecules, though slight variations in the intramolecular bond lengths and rotations of the methyl and hydroxyl groups on the alocohol molecule are permitted; that is, the molecules are not rigid. These fundamental structural constraints in conjunction with the fixed atomic density of the model prevent the EPSR procedure from becoming too sensitive to the systematic errors, primarily neutron scattering inelasticity effects in the experimental data and that are known to be manifest on the short length scales <3 Å. This model box was then allowed to develop under standard Monte Carlo procedures but subject to a periodic perturbation to the reference potentials via a potential of mean force derived from the experimental diffraction data: $\psi_{\alpha\beta}(r) = -kT \ln(g_{\alpha\beta}(r))$. With each iteration and subsequent perturbation, the intermolecular structure represented by the simulation box of molecules is driven into closer agreement with the measured partial structure factors in the range 0.3−30 Å^{-1}. Once satisfactory agreement is reached, i.e., that the structure factors calculated from an instantaneous snapshot of the molecular configurations match the experimental data and that the Fourier transform of the fit residual is seen to match the data in the intermolecular length scales of interest >3 Å, accumulation of the box configurations is commenced. These configurations are

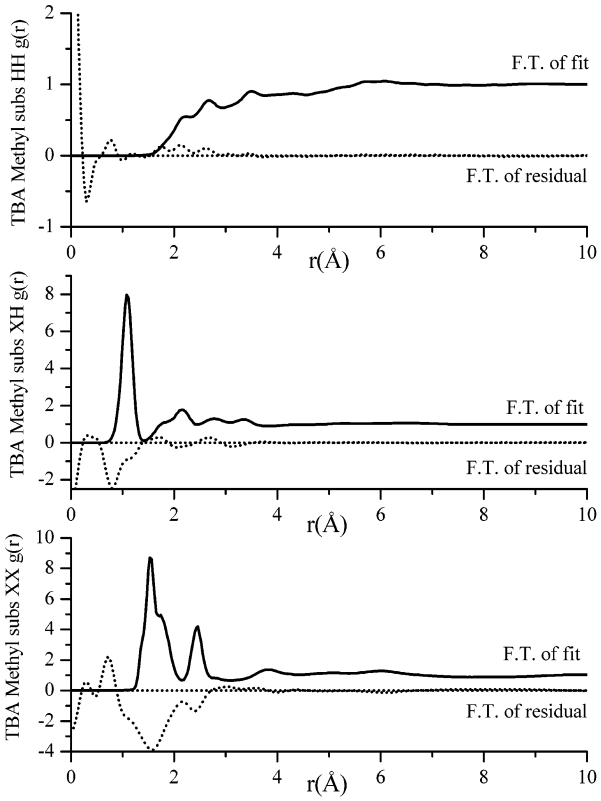

Figure 2. Composite radial distribution functions (solid lines) $g_{HH}(r)$, $g_{XH}(r)$, and $g_{XX}(r)$ derived by the EPSR method from the data and model fits shown in Figure 1. Also shown are the Fourier transforms of the fit residuals (broken lines). These illustrate that the fits have captured the essence of the data on the intermolecular length scales >3 Å.

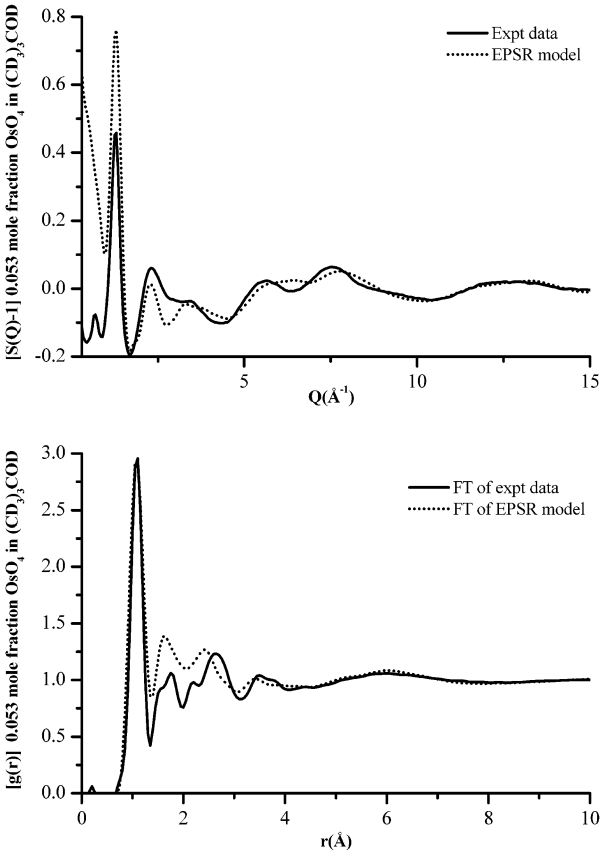

Figure 3. Comparison of how the EPSR model compares with the total structure factor $F(Q)$ measured for the 0.053 mole fraction solution of OsO_4 in $(CD_3)_3COD$ (top panel). The corresponding comparison between the pair distribution functions derived from these total structure factors are shown in the bottom panel. The experimental data have not been corrected for any inelastic scattering component at this stage, but again we note that the most significant differences between the model and the experimental data occur below 3 Å in the region of the intramolecular structural correlations of the tertiary butanol molecules.

then analyzed and stored, and ensemble averaged structural functions are thus generated. In this study, ≈21 000 box configurations were accumulated.

The model constraints imposed by maintaining the intramolecular structure and atomic density of the system have been found to be extremely effective at compensating for systematic effects in the data.[17] These recent tests of the EPSR procedure show that the same structural conclusions are drawn even when utilizing independent input data sets (on the same systems under the same thermodynamic conditions) but collected under a wide range of instrumental conditions and over a long period of time.[17] Furthermore a comparison of the results obtained from earlier alcohol−water studies[9,10] has shown that the intermolecular structural picture generated by the procedure is robust to the number and type of isotopic substitution experiments performed, provided the selection of substitutions is sufficient to capture the dominant structural correlations between the principal molecular component. The additional constraints imposed on the model by the generated network of the principal molecular component of the mixture limit the possibilities for the structural incorporation of the minor component into the model. The strongly weighted terms in the experiment thus enhance the determination of the weaker molecular interactions beyond the simple estimate provided by the table of neutron scattering weights (Table 1).

Results

(A) Experiment and EPSR Model. In Figure 1, we show the three composite partial structure factors derived from the three isotopic measurements, namely, $S_{HH}(Q)$, $S_{XH}(Q)$, and $S_{XX}(Q)$. Also shown is the EPSR model fits and fit residuals to the experimental data. We note that the agreement between the model and fits is generally good for the $S_{HH}(Q)$ and $S_{XH}(Q)$ functions, though at $Q < 2.5$ Å^{-1} the fit to the $S_{XX}(Q)$ data is not perfect though the salient features and oscillations are present. This mismatch is due to the residual inelasticity components that were not perfectly removed by the correction procedures.[12] In general, the problem is most challenging to solve for this third function as the small residual errors in the experimental separation of the partial structure factors tend to accumulate in $S_{XX}(Q)$. As mentioned above, to overcome this, we take advantage of the strengths of the EPSR data analysis scheme, in particular that basic systematic constraints such as the atomic density and intrinsic molecular geometries can be imposed during the model building process. These constraints help to minimize the effects of residual errors on the final models, and Fourier analysis of the fit residual shows that the observed deviations of the fit do not introduce significant structural perturbations to the derived model on the intermolecular length scales of interest.

In Figure 2, we show the composite partial distribution functions corresponding to the Fourier transform of the partial structure factors of Figure 1 and Fourier transforms of the fit residuals. The transforms of the fit residuals show that beyond ∼3 Å, corresponding to the start of the intermolecular length scales of interest, the models have captured the essence of the experimental data and have not introduced large deviations in

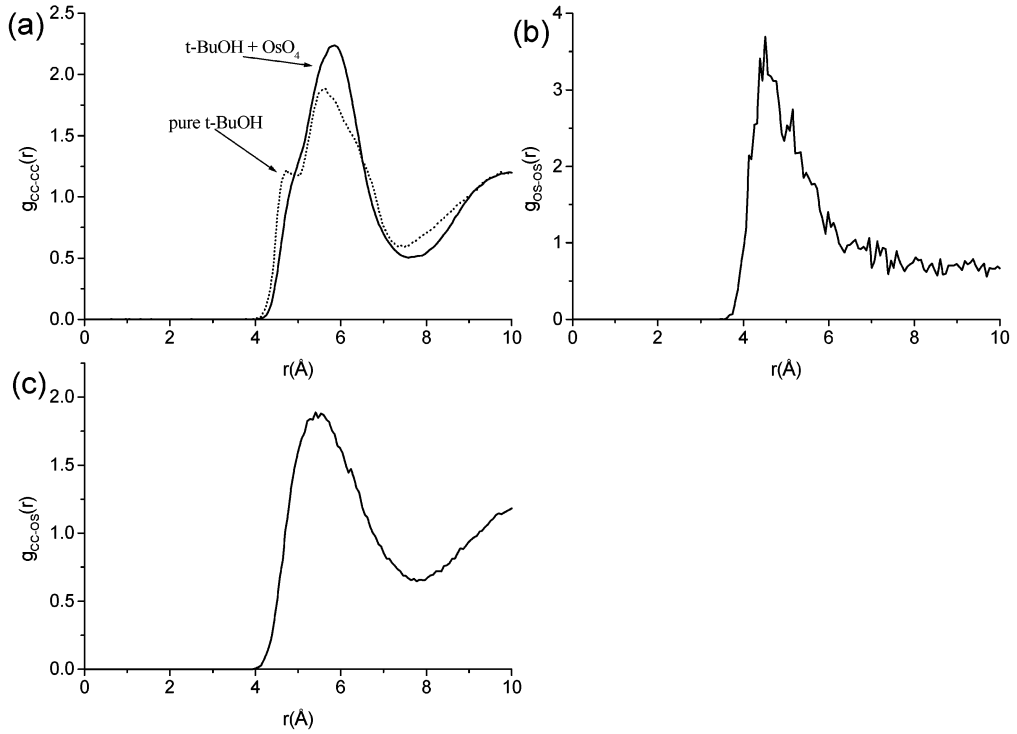

Figure 4. Molecular centers partial pair distribution functions (a) $g_{CC-CC}(r)$, (b) $g_{OS-OS}(r)$, and (c) $g_{CC-OS}(r)$ derived for the 0.053 mol fraction OsO_4 in tertiary butanol solution (solid lines). The alcohol molecular centers function [(a) $g_{CC-CC}(r)$] is compared with the analogous function obtained for the pure alcohol that and shown as the broken line.[4]

this range. The deviations in the short range are due to the difficulty in accurataely performing the corrections for inelastic scattering of the neutrons, which is a particular challenge for the light hydrogen containing samples.[12] Because of the complex mixture of atomic pair contributions contained in $g_{XH}(r)$ and $g_{XX}(r)$, these functions are difficult to interpret meaningfully (see the weightings given in Table 1). In this case, the function $g_{HH}(r)$ is also difficult to interpret because of the spatial averaging that occurs which is due to the distribution of nine identical methyl hydrogen sites on the alcohol molecule. It is these difficulties that led us to adopt the EPSR data analysis scheme for these data.

As a final comparison of the EPSR model with the experimental data, Figure 3 shows the total structure factor $F(Q)$ calculated from the EPSR model for the fully deuterated alcohol solution of OsO_4 (solution 3). This is compared with the experimental data on this sample though we note that at this stage these experimental data are not corrected for inelastic scattering as this correction is performed in the process of generating the partial structure factors[12] shown in Figure 1. The corresponding Fourier transforms of these total structure factors, also shown in Figure 3, again demonstrate that the most significant differences between the model and the experimental data occur in the distance ranges that correspond to the intramolecular, rather than intermolecular, structure of the alcohol molecules.

(B) Partial Structure Factors. Figure 4 parts a−c shows the molecular centers partial distribution functions derived from the EPSR model of the solution. Figure 4a shows the alcohol−alcohol tertiary carbon site correlations and compares them with the same correlation function previously determined for the pure alcohol system. It is immediately obvious that the nature of the alcohol−alcohol interactions is perturbed by the presence of the osmium tetroxide molecules in the system, even though the concentration of these molecules is relatively dilute with 18 alcohol molecules for each OsO_4. The main effect appears to be a shift in the principal maximum of the function from 5.6 to 5.8 Å and a softening of the shoulder that appears at 4.8 Å in the $g_{CC-CC}(r)$ for the pure alcohol. In the mixture system, this shoulder is merged into the main peak at ∼5 Å. The previous investigation of the pure alcohol system[4] showed that this shoulder in the $g_{CC-CC}(r)$ function is characteristic of the interalcohol hydrogen bonding that occurs in the system.

TABLE 2: Coordination Numbers Obtained by Integration of the Features in the Indicated Partial Distribution Functions

correlation	atomic density ρ (atom Å^{-3})	R_{min} (Å)	R_{max} (Å)	coordination number (atoms)
CC−CC	0.0064	4.0	5.0	0.9 ± 0.1
		4.0	7.0	10.1 ± 0.4
		4.0	7.5	11.3 ± 0.4
		5.0	7.5	10.5 ± 0.4
CC−OS	0.0004	4.0	7.75	0.7 ± 0.1
OS−CC	0.0064	4.0	7.75	11.9 ± 0.1
M−OO	0.0014	2.1	4.5	0.3 ± 0.02
		4.5	7.5	1.9 ± 0.04
OS−OS	0.0004	3.5	6.0	0.5 ± 0.4
O−O	0.0064	2.4	3.35	1.1 ± 0.1
		2.5	3.5	1.3 ± 0.2
O−D	0.0064	1.2	2.8	0.6 ± 0.1
		2.8	5.0	2.1 ± 0.1
		2.9	4.0	1.2 ± 0.1
D−D	0.0064	1.8	4.0	2.2 ± 0.2
O−OS	0.0004	3.0	5.75	0.3 ± 0.1
		5.75	8.0	0.4 ± 0.1
		3.0	8.0	0.7 ± 0.1
O−OO	0.0014	2.6	4.5	0.4 ± 0.1
		4.5	7.0	1.5 ± 0.1
OS−O	0.0064	3.0	5.75	4.9 ± 0.9
		5.75	8.0	8.1 ± 1.1
		3.0	8.0	13.0 ± 1.5
D−OS	0.0036	2.0	6.0	0.3 ± 0.1
D−OO	0.0014	1.8	4.5	0.4 ± 0.1
		4.5	7.5	1.9 ± 0.1
OS−D	0.0064	2.0	6.0	5.7 ± 1.0

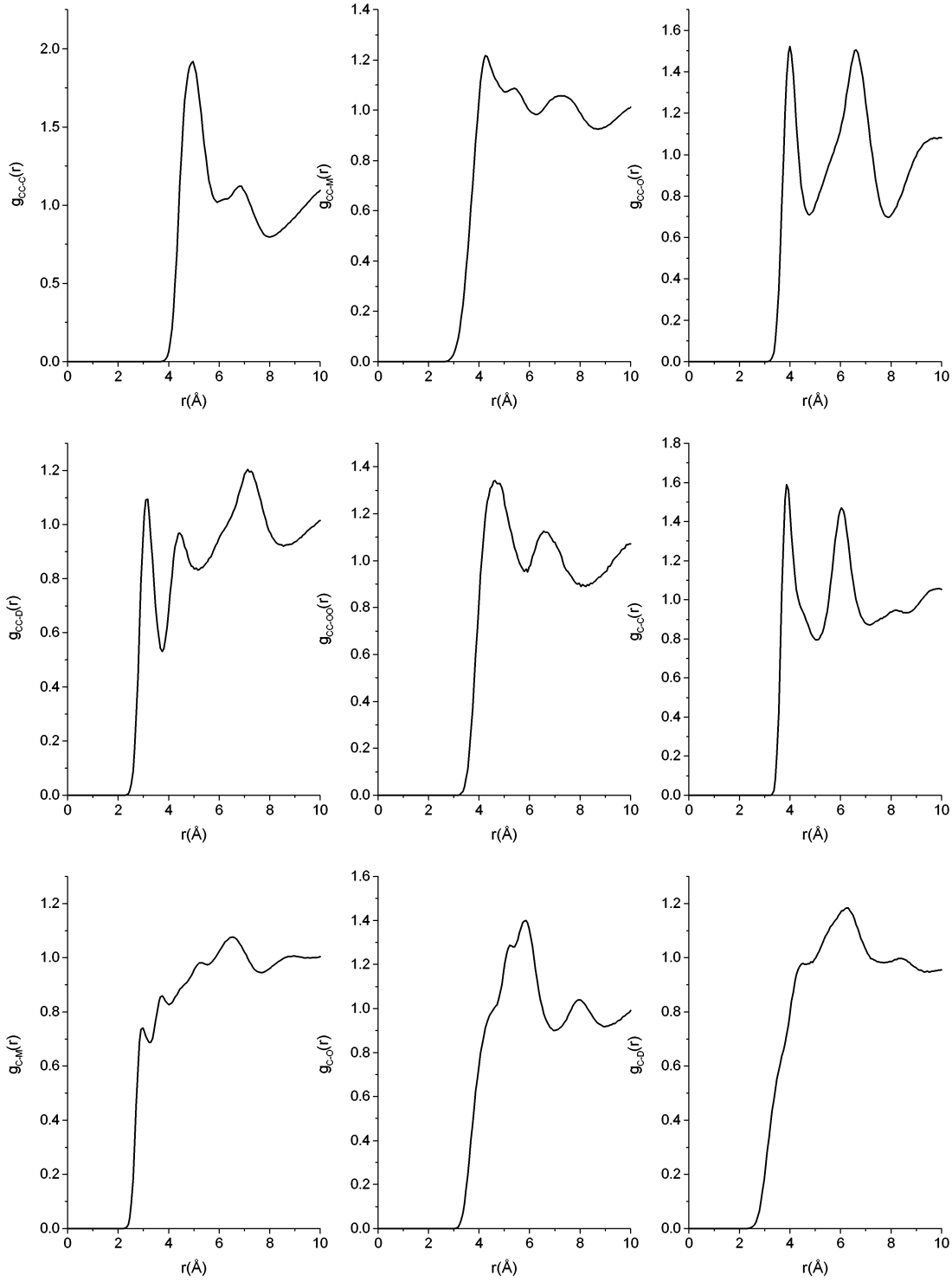

Figure 5. Intermolecular partial distribution functions derived by the EPSR procedure 1: CC−C, CC−M, CC−O, CC−D, CC−OO, C−C, C−M, C−O, and C−D for a 0.053 mol fraction OsO_4−tertiary butanol solution at room temperature.

Consequently, the change in this feature observed here indicates that in some way the OsO_4 molecules are modifying these interactions and pushing them to longer distances. It is worth stating that although the alcohol molecule hydroxyl group sites have not been explicitly substituted in this study, earlier experience with alcohol−water systems[9,10] has shown that the selected isotopic substitutions performed here, in conjunction with EPSR technique, still enables us to capture the essence of these correlations in a reliable fashion. The integral between 4 and 5 Å (Table 2) in the mixed system shows a coordination number of 0.9 ± 0.1, which is very comparable with the value of 1.2 ± 0.2 obtained for the pure alcohol system; that is, each alcohol molecule is on average hydrogen bonded to one other alcohol molecule. Together these findings suggest that OsO_4, although modifying the interalcohol hydrogen bonding interaction, does not change its quantitative extent. The integral of the function between 5 and 7.5 Å shows that in this distance range the number of alcohol−alcohol interactions is increased over the pure liquid from a value of 9.6 ± 0.5 to 10.5 ± 0.4.

Figure 4b illustrates the correlations between the OsO_4 molecules and themselves. Because of the dilute nature of this species in the mixture, the function displays considerably more

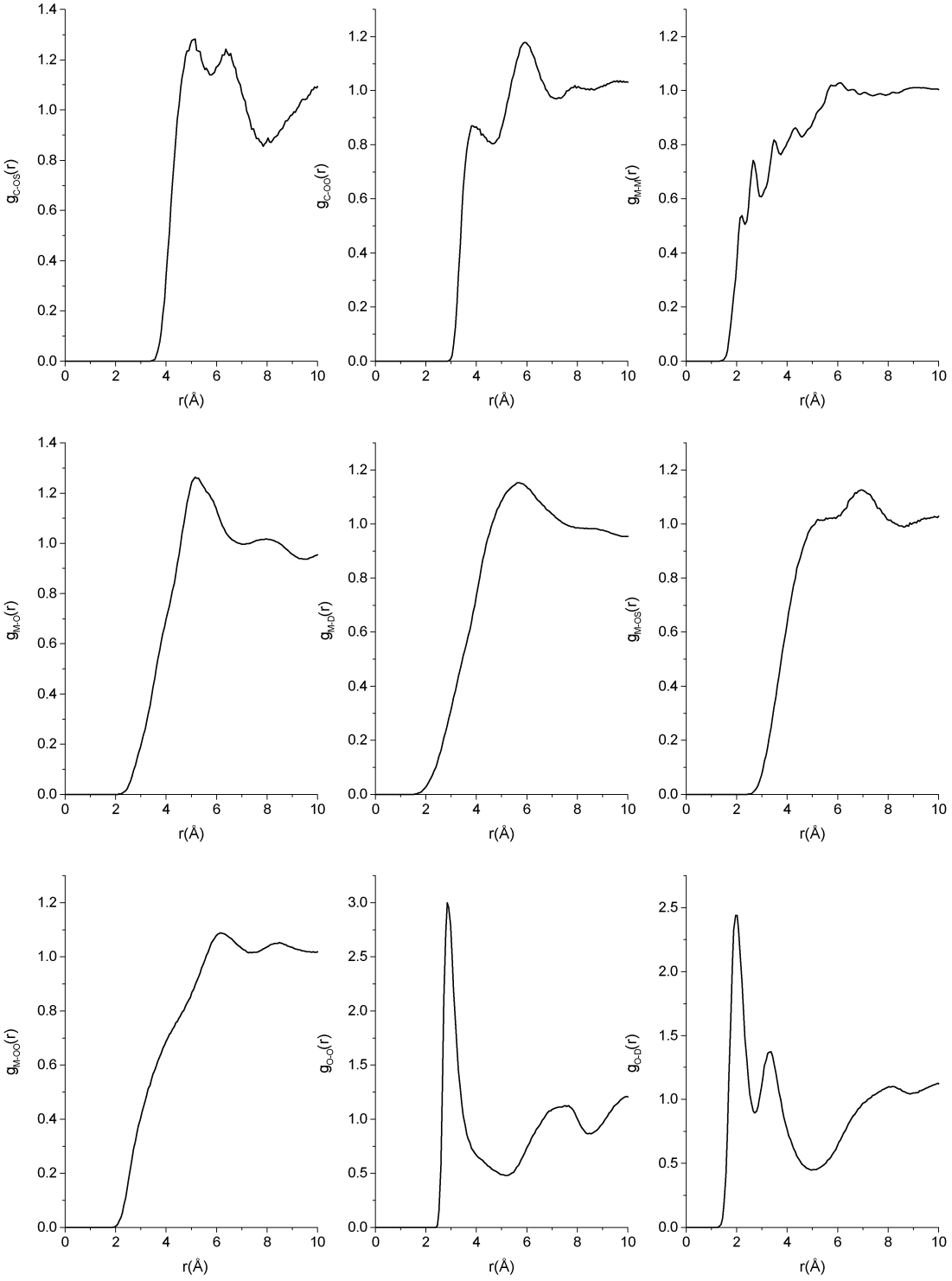

Figure 6. Intermolecular partial distribution functions derived by the EPSR procedure 2: C−OS, C−OO, M−M, M−O, M−D, M−OS, M−OO, O−O, and O−D for a 0.053 mol fraction OsO_4−tertiary butanol solution at room temperature.

noise, though the main features and magnitude of the correlations are clearly determined. The function peaks at 4.5 Å (Table 2) and gives a coordination number in the 3.5−6 Å range of 0.5 ± 0.4 neighboring osmium atoms. This is indicative that by and large the osmium tetroxide molecules in this system are most often found as isolated molecules and less frequently in pairs or higher numbers. The alcohol thus appears to be a good medium in which this molecule can be dispersed.

Figure 4c shows the molecular centers cross correlation function between the alcohol molecules and OsO_4. The favored distance of interaction can be seen to be ∼5.5 Å with the coordination numbers indicating that on average each alcohol molecule has 0.7 ± 0.1 OsO_4 molecules at this distance, whereas in turn, each OsO_4 is surrounded by 11.9 ± 0.1 alcohol molecules.

For completeness, Figures 5−7 show the remaining 25 partial pair distribution functions that fully characterize the range of interactions that occur in the mixture of alcohol molecules and osmium tetroxide molecules. The relatively prominent peaks at a similar distance of 4.5 Å in the $g_{O-OS}(r)$ and $g_{D-OS}(r)$ (Figure 7) illustrate that the OsO_4 molecules are found in the vicinity of the polar hydroxyl group of the alcohol. However,

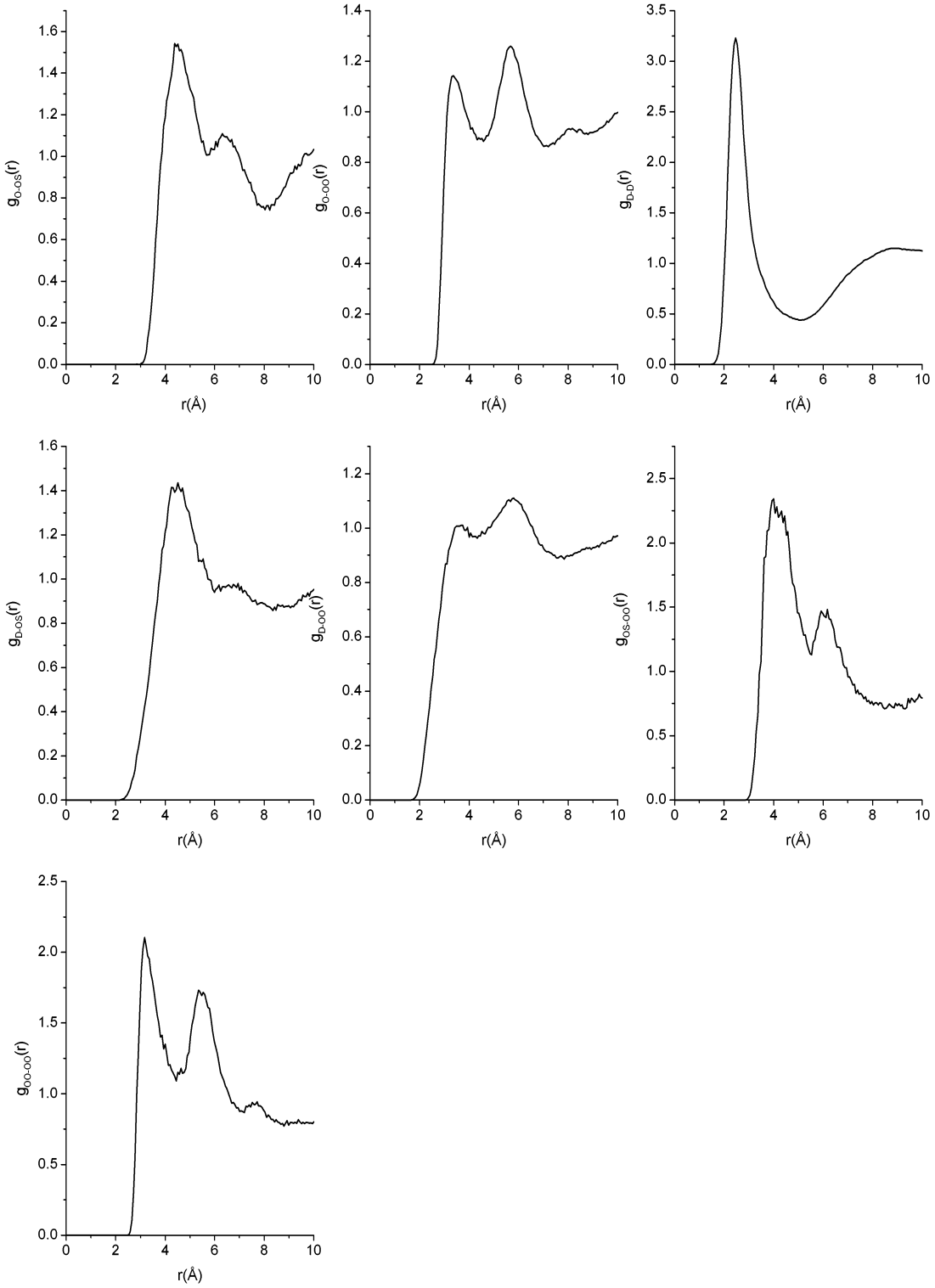

Figure 7. Intermolecular partial distribution functions derived by the EPSR procedure 3: O−OS, O−OO, D−D, D−OS, D−OO, OS−OO, and OO−OO for a 0.053 mol fraction OsO_4−tertiary butanol solution at room temperature.

the similarity in form of these two functions shows that the interaction is unbiased with regards to any preference for oxygen or hydrogen atom coordination and is thus consistent with the OsO_4 molecule not actively bonding to the polar group of the alcohol. This can be further corroborated by the study of the functions $g_{O-OO}(r)$ and $g_{D-OO}(r)$ (Figure 7). The first peak in both functions indicates that the OsO_4 molecules do come into direct contact with this group without a given preference. The coordination number for $g_{O-OO}(r)$ and $g_{D-OO}(r)$ in the range up to 4.5 Å, corresponding to the first peak at 3.4 Å, is directly comparable to that obtained for the first peak in $g_{O-OS}(r)$ and $g_{D-OS}(r)$. This suggests that the coordination of the OsO_4 molecule is directly made via one of the four oxygen atoms and not through a tetrahedral face.

A comparison of $g_{O-OO}(r)$ and $g_{D-OO}(r)$ with $g_{M-OO}(r)$ (Figure 6) shows that the OsO_4 molecules that do coordinate with methyl group hydrogen atoms do so from their localized position close the alcohol hydroxyl group. In the latter function,

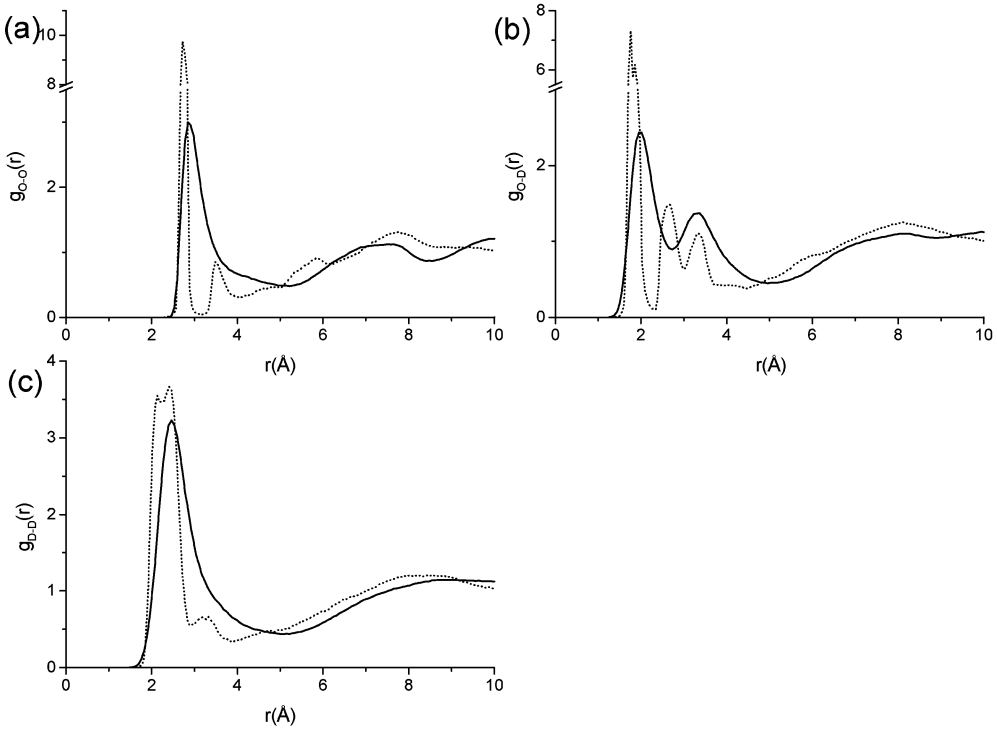

Figure 8. Intermolecular partial distribution functions corresponding to alcohol−alcohol hydrogen bonding correlations between the alcohol molecule hydroxyl groups, (a) $g_{O-O}(r)$, (b) $g_{O-D}(r)$, and (c) $g_{D-D}(r)$, in a 0.053 mol fraction OsO_4−tertiary butanol solution at room temperature (solid lines). These functions are compared with the same functions obtained for the pure liquid alcohol (broken lines).[4]

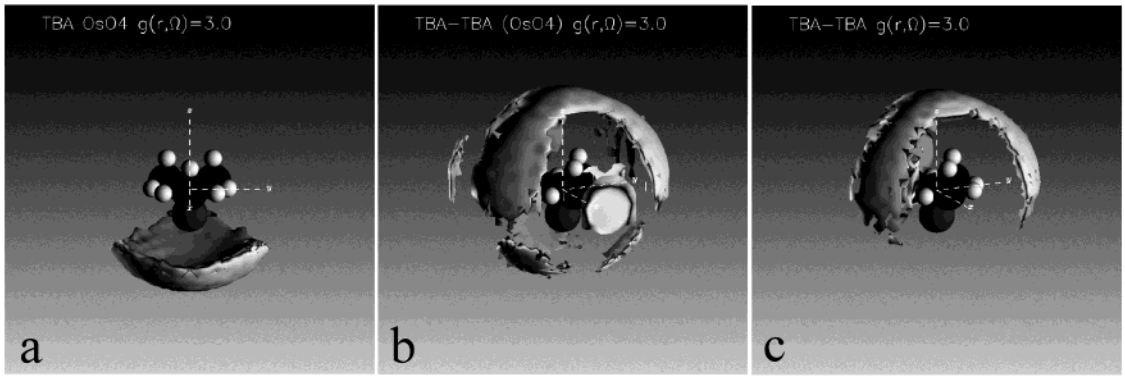

Figure 9. Spatial density functions (a) $g_{CC-OS}(r,\Omega)$ for a 0.053 mol fraction OsO_4−tertiary butanol solution at room temperature, (b) $g_{CC-CC}(r,\Omega)$, for a 0.053 mol fraction OsO_4−tertiary butanol solution at room temperature, and (c) $g_{CC-CC}(r,\Omega)$ for a 0.14 mol fraction water in tertiary butanol solution at room temperature.[16] All functions were derived by EPSR modeling procedures. This function represents a three-dimensional map of the favored regions for finding an OsO_4 molecule around an alcohol molecule (a) or finding an alcohol molecule around another alcohol molecule (b and c), as a function of radial distance, r, and orientation, Ω. The viewports in each case are centered on and scaled to the alcohol central carbon atom ±10 Å. In each case, the probability level for the iso surface is set to highlight the preferable directions of first neighbor correlations. Together, these figures summarize the dominant interactions between the molecular species in solution. First, the strong preference of the OsO_4 molecules to sit just below the alcohol hydroxyl group region and, second, the mix of nonpolar group to nonpolar group (b and c) and hydrogen bonding interactions (b) that occur between alcohols.

$g_{M-OO}(r)$, the most favorable interaction distance can be seen to be 6.2 Å, which is a distance that does not correspond to localization around the nonpolar end of the alcohol molecules. Corresponding coordination numbers are given in Table 2. Through their preference for the region of space close to the alcohol hydroxyl groups, these OsO_4 molecules will undoubtedly have an impact on the hydrogen bonding interactions that occur between the alcohol molecules. The details of this are shown in Figure 8 through a comparison with the alcohol hydroxyl group correlations obtained for the pure alcohol system.

Figure 8a shows us that the presence of the OsO_4 molecules considerably reduces the degree of order in the inter-hydroxyl-group oxygen correlations $g_{O-O}(r)$, broadening the first peak by more than a factor of 2 and moving the position of the maximum from 2.7 to 2.9 Å. Interestingly, however, the coordination number integrated between 2.4 and 3.35 Å remains unchanged in the two systems with a value of 1.1 ± 0.2 hydroxyl oxygen neighbors and confirming the findings suggested by our examination of the features in the $g_{CC-CC}(r)$ distribution function. Figure 8b,c further emphasizes the trend of OsO_4 to increase the disorder present in the interalcohol hydrogen bonding interactions with the peaks in both the $g_{O-D}(r)$ and $g_{D-D}(r)$ being considerably broadened and the function maxima displaced to larger distances.

(C) Spatial Density Functions. Figure 9 shows the spatial density functions calculated for the t-BuOH−OsO_4 (8a) and

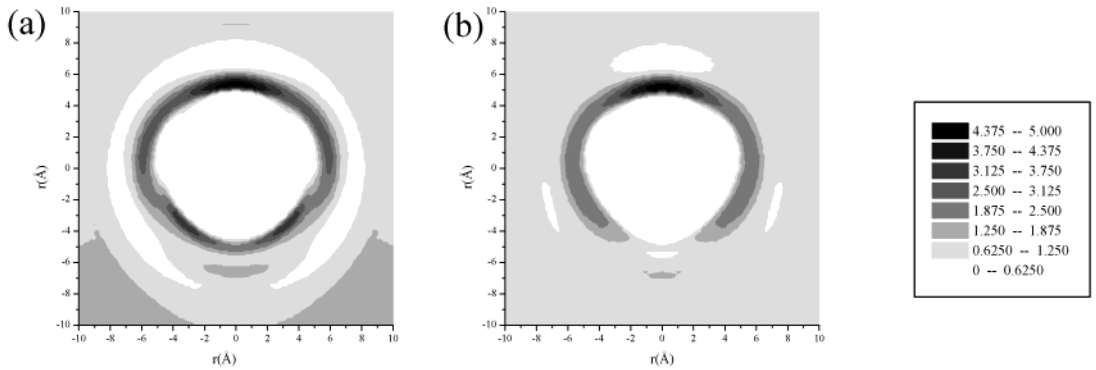

Figure 10. Illustration of the orientational correlation maps produced by averaging parts a and b of Figure 8 over rotations around the axis defined by the central carbon and hydroxyl group oxygen of the central alcohol molecule. This figure illustrates how in contrast to the case for an 0.14 mol fraction water in tertiary butanol solution (b), the hydrogen bonding between alcohol molecules is preserved in the 0.053 mol fraction OsO_4 in tertiary butanol mixture (a). This is made visible by the presence of the lobes of intensity in the 5 and 7 o'clock directions in panel a that are absent in panel b.

alcohol−alcohol (8b) correlations. These plots highlight the regions of favorable first neighbor contacts by showing the distribution of molecular centers about an arbitrary alcohol molecule. Figure 9a shows us that the preferred location of an OsO_4 molecule near a tertiary butanol molecule is indeed in the region below the alcohol hydroxyl group. This confirms the hypothesis that was built from our examination of the partial structure factors. As the OsO_4 molecules are localized in this very specific spatial region in relation to the alcohol molecules, it is easy to understand why their presence might affect the distribution of the hydrogen bonding. Because OsO_4 is not capable of forming hydrogen bonds itself, it does not however suppress the interalcohol bonds but rather works to modify their spatial distribution from that which is found in the pure liquid alcohol (Figure 8). This picture can be clarified by examining the alcohol-alcohol spatial density function.

In Figure 9b, it is clear that the bulk of the alcohol−alcohol interactions in the alcohol−OsO_4 mixture occur in the directions that would be mediated by the nonpolar methyl groups, though three lobes corresponding to interalcohol hydrogen bonding interactions are visible in the lower half of the figure. To emphasize the extent, to which the non-hydrogen-bonding OsO_4 molecules can be incorporated into the alcoholic solvent without disrupting the alcohol-alcohol hydrogen bond network, it is interesting to compare this figure with one obtained for a system in which a hydrogen bond forming molecule is added. In Figure 9c, we illustrate the spatial density function that is generated for the case where 0.14 mol fraction of water is present in tertiary butanol solution. In this comparison mixture, it is clear that the majority of the hydrogen bonding interactions between the alcohol molecules have been suppressed, though the methyl group mediated interactions appear broadly similar. This change in the nature of the intermolecular interactions can be seen vividly in the orientational correlation plots shown in Figure 10. This plot is effectively a two-dimensional rendering of parts b and c of Figure 9, averaged over rotation of the central molecule about the axis defined by the central carbon, CC, and the hydroxyl group oxygen, O. Figure 10a shows the map calculated for the t-BuOH−OsO_4 system, and Figure 10b shows the corresponding map for a 0.14 mol fraction water in t-BuOH mixture. The absence of the lobes in the 5 o'clock and 7 o'clock directions of Figure 10b is indicative of the suppression of the interalcohol hydrogen bonding correlations that the addition of water produces. In contrast, Figure 10a confirms that OsO_4 can be accommodated in the alcohol solution with less disruption to this aspect of the alcohol molecule interactions.

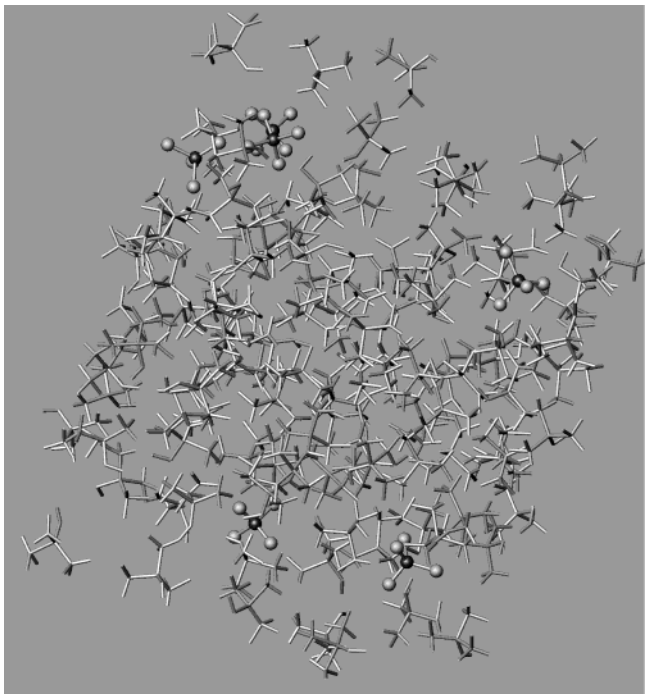

Figure 11. Snapshot of the EPSR model box used in the refinement of the structure of a 0.053 mol fraction OsO_4 in tertiary butanol solution. The figure illustrates the full cubic box of side length 25.6 Å containing 108 tertiary butanol molecules and 6 OsO_4 molecules. By and large, the OsO_4 molecules are dispersed individually throughout the mixture, thought occasionally small clusters of this molecule do occur.

Conclusions

The results obtained from the EPSR modeling of the isotopic substitution neutron diffraction data allow us to produce a structural picture of a 0.053 mol fraction OsO_4 in t-BuOH solution in which the osmium molecules are well dispersed among the alcohol molecules. The local environment favored by the OsO_4 molecules within the liquid are the spatial regions close to the alcohol hydroxyl groups, with each OsO_4 molecule on finding on average 13.0 ± 1.0 alcohol hydroxyl groups between 3.0 and 8.0 Å.

Though the OsO_4 molecules are located in close proximity to the polar hydroxyl groups of the alcohols, they appear not to suppress the interalcohol hydrogen bonding that occurs. This is found to be quantitatively similar in extent to that found in the pure liquid alcohol. However, the presence of the OsO_4 in this spatial position relative to the alcohol molecules does appear

to contribute to an increase in the intrinsic disorder in the hydrogen bonding interactions between the alcohol molecules. This appears to occur through a slight lengthening of the interalcohol hydrogen bonds by ~0.2 Å and an increase in the breadth of their distribution.

To summarize, the solution state of this OsO_4−alcohol mixture is illustrated in Figure 11 through a snapshot taken of the EPSR model box during data refinement. This figure illustrates that the OsO_4 molecules are generally well dispersed as individual molecules within the solution, though that occasionally they do come together in small aggregates. The coordination number analysis discussed earlier however, tells us that this formation of small clusters is generally uncommon and that the preferred state of the solute is to be individually solvated by up to 13 alcohol molecules.

References and Notes

(1) Riemersma, J. C. *Biochim. Biophys. Acta* **1968**, *152*, 718.
(2) Jacobsen, E. N.; Marko, I.; Mungall, W. S.; Schroder, G.; Sharpless, K. B. *J. Am. Chem. Soc.* **1988**, *110*, 1968.
(3) Kolb, H. C.; VanNieuwenhze, M. S.; Sharpless, K. B. *Chem. Rev.* **1994**, *94*, 2483.
(4) Bowron, D. T.; Finney, J. L.; Soper, A. K. *Mol. Phys.* **1998**, *93*, 531.
(5) Bowron, D. T.; Finney, J. L.; Soper, A. K. *Mol. Phys*. **1998**, *94*, 249.
(6) Kusalik, P. G.; Lyubartsev, A. P.; Bergman, D. L.; Laaksonen, A. *J. Phys. Chem. B* **2000**, *104*, 9526.
(7) Jorgensen, W. L. *J. Phys. Chem*. **1986**, *90*, 1276.
(8) Gao, J.; Habibollazadeh, D.; Shao, L. *J. Phys. Chem*. **1995**, *99*, 6208.
(9) Bowron, D. T.; Finney, J. L.; Soper, A. K. *J. Phys. Chem. B*. **1998**, *102*, 3551.
(10) Bowron, D. T.; Soper, A. K.; Finney, J. L. *J. Chem. Phys.* **2001**, *114*, 6203.
(11) Soper, A. K.; Howells, W. S.; Hannon, A. C. *ATLAS—Analysis of Time-of-Flight Diffraction Data from Liquid and Amorphous Samples*; Rutherford Appleton Laboratory Report RAL 89-046; Rutherford Appleton Laboratory: U.K., 1989.
(12) Soper, A. K.; Luzar, A. *J. Chem. Phys*. **1992**, *97*, 1320.
(13) Soper, A. K. *Chem. Phys.* **1996**, *202*, 295.
(14) Soper, A. K. *Mol. Phys.* **2001**, *99*, 1503.
(15) Soper, A. K. *J. Chem. Phys.* **1994**, *101*, 6888.
(16) Svishchev, I. M.; Kusalik, P. G. *J. Chem. Phys.* **1993**, *99*, 3049.
(17) Soper, A. K. *Chem. Phys.* **2000,** 258, 121.